Available online at www.sciencedirect.com

SCIENCE DIRECT

Surface & Coatings Technology 200 (2005) 730–733

SURFACE & COATINGS TECHNOLOGY

www.elsevier.com/locate/surfcoat

MicroFabrication of flow field channels in glassy carbon by a combined laser and reactive ion etching process

M. Kuhnke, T. Lippert*, G.G. Scherer, A. Wokaun

Electrochemistry Laboratory, Paul Scherrer Institut, 5232 Villigen, Switzerland

Available online 19 March 2005

Abstract

Micro structuring of glassy carbon (GC) can be performed by various methods such as sawing, laser ablation, and reactive ion etching (RIE). Our combined laser and reactive ion etching process comprises a laser mask writing step in a sputter-deposited metal layer and a pattern transfer step performed by reactive ion etching. The laser mask writing is achieved by a XeCl laser (308 nm) and a computer controlled setup that allows flexible variation of the pattern. The layout input from plotter files (HPGL) and the writing speed of up to 1 mm/s make this method suitable for rapid prototyping. Subsequent reactive ion etching in oxygen plasma results in channels with trapezoid cross-section, a depth of ~100 μm, and aspect ratios ~1.5. A complete flow field with a size of 1 cm^2, consisting of 5 meandering channels with a depth of 72 μm and a top width of 59 μm, was prepared for micro fuel cell operation.

Keywords: Glassy carbon; Micro fuel cell; Laser ablation; Metal film; Reactive ion etching

1. Introduction

Fuel cells are a promising technology for energy conversion and have recently gained attention in the sector of small power supplies for portable applications such as notebooks, camcorders, and cell phones. For these applications, a miniaturized cell design was developed that reduces the number of components and simplifies manufacturing and assembly. Alternative techniques for micro fuel cell (μFC) fabrication are usually based on silicon/glass technology and conventional carbon-supported platinum electrodes [1–6] or screen printed electrodes [7]. These cells are usually fabricated co-planar and have the main disadvantage of the high resistivity of silicon. Other groups fabricate μFCs based on thick film printing technology on alumina substrates [8] or PCB (printed circuit board) technology [9].

Our approach is the fabrication of a micro fuel cell electrode in glassy carbon (GC, Sigradur® G, pyrolyzed at 2200 K), which exhibits a high electrical conductivity and chemical inertness. The electrode consists of a channel structure with typical dimensions of 50 μm width and ~100 μm depth. This flow field provides the gas supply, a support for the electrocatalyst, and is a perfect system to study the mechanisms that determine catalyst utilization [10].

Several techniques for the fabrication of structures in GC have been studied in our group and by other groups. The methods vary from sawing and laser direct writing [11,12] to reactive ion etching (RIE) with SiO_2 masks [13], anodic etching with resist mask [14,15] and mold and bake techniques in polymers [16,17]. A novel method for the structuring of glassy carbon is the combination of a laser ablation step with subsequent reactive ion etching. The process has been described in detail elsewhere [11], but briefly: a metal layer is deposited on the glassy carbon and structured by laser ablation, in order to create a mask for the reactive ion etching step. The pattern of this mask is then transferred into the glassy carbon substrate by a RIE step in oxygen plasma.

* Corresponding author: Tel.: +41 56 310 4076; fax: +41 56 310 2688.
E-mail addresses: markus.kuhnke@psi.ch (M. Kuhnke), thomas.lippert@psi.ch (T. Lippert).

0257-8972/$ - see front matter © 2005 Elsevier B.V. All rights reserved.
doi:10.1016/j.surfcoat.2005.01.096

2. Experiment

One of the most important factors of this process is the good adhesion of the metal mask on the GC surface. Therefore, several pretreatment methods were tested [11] and the best results were obtained after mechanical polishing with diamond paste (6 μm). The aluminum layers with a thickness of 400 or 600 nm were sputter-deposited onto the glassy carbon samples.

Laser structuring of the Al layer was performed with a XeCl (308 nm) excimer laser at fluences of ~3–4 J cm^{-2}. Circular spots with a size of 25–40 μm were ablated by imaging a pinhole with a lens (f=10 cm) on the sample surface. The sample was mounted on a computer controlled xyz stage while the position of the laser beam was kept constant.

The control software was programmed in LabView and allows the import of patterns as plotter files (HPGL). In addition to single axis moving, both linear interpolated (diagonal) moves and circular moves can be performed by the motorized xyz stage. Patterns are written pulse by pulse with an adjustable step width and velocities up to 1 mm/s (at 20 μm step width and 50 Hz laser repetition rate).

For the reactive ion etching of GC an Alcatel GIR300 with a capacitively coupled 6-inch electrode, a maximum RF power of 600 W and a pressure range of 5–100 mTorr ($6.7 \cdot 10^{-3}$–$1.3 \cdot 10^{-1}$ mbar) was applied. The RF electrode can be covered by a glass or a stainless steel plate, which results in different sputtering characteristics. Glassy carbon is etched in oxygen plasma and the gaseous products CO_2 and CO are removed by the vacuum pumps.

The remaining Al mask is subsequently removed by ultrasonic cleaning in de-ionized water, where it peels off within a few seconds due to mechanical stress in the layer. In this process step, the brittle "grass" in the channels, formed during the RIE step (see Section 3.3), is also removed completely.

3. Results and discussion

3.1. Improvement of metal adhesion

Polishing the glassy carbon with abrasive diamond paste (6 μm) was identified as the most reliable method to obtain a good adhesion of the Al layer. Other techniques such as reactive ion etching in reactive and non-reactive gases (Ar, N, O_2) or the use of a Cr interlayer did not result in equally good adhesion. This is different to the case of copper films on GC, where an improved adhesion could be obtained by nitrogen plasma treatment [18] or by using a chromium interlayer of 2–10 nm thickness [19]. Another important parameter for the adhesion seems to be the base pressure before sputtering the Al layer onto the glassy carbon at $3 \cdot 10^{-3}$ mbar. Several samples exhibited "bubble" formation (Fig. 1) during the reactive ion etching process. The base pressure in this case was $5 \cdot 10^{-5}$ mbar, while at base pressures of $< 8 \cdot 10^{-6}$ mbar, no bubble formation occurred. Therefore, we assume that gas or water adsorbed at the rough GC surface might not desorb sufficiently at pressures of $\geq 5 \cdot 10^{-5}$ mbar. The adsorbed gas would expand during the reactive ion etching process, when the samples reach temperatures above 50 °C at a pressure of ~50 mTorr ($6.6 \cdot 10^{-2}$ mbar).

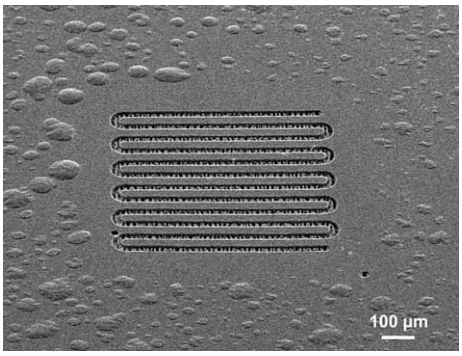

Fig. 1. "Bubbles" formed between GC and Al layer after reactive ion etching.

3.2. Laser mask writing

Laser ablation of the aluminum layer at an irradiation wavelength of 308 nm can be achieved by single spot irradiation. For a layer thickness of 400 nm, a fluence of 2.5– 3 J/cm^2 is required, while for 600 nm, 3.5–4.0 J/cm^2 is necessary. Overlapping spots reduce the number of aluminum droplets remaining in the ablated area. In all cases, several hundred nanometers of GC are also ablated from the substrate (about 1 μm for 600 nm Al mask with 3.5 J/cm^2 and 10 μm steps).

The step width, which can be adjusted to ≥0.1 μm, determines the edge roughness of the written lines. At a spot diameter of 30 μm, a step width of 10 μm is sufficient for an edge roughness of ~1 μm. Depending on the laser repetition rate, which can be varied from 1–50 Hz, writing speeds of 0.1–1000 μm/s are feasible.

Variable mask layouts can be written by using HPGL files. All mask layouts are drawn ten times larger and then scaled down by the control software, which corresponds to a resolution of 2.5 μm. For even higher resolution, larger scaling factors can also be used. Examples of laser-written linear and circular patterns are shown in Fig. 2.

3.3. Reactive ion etching

The pattern transfer step in oxygen plasma was optimized for high etch rates by varying the power and the pressure (Fig. 3). The maximum etch rate of 40 μm/h was achieved at 100 mTorr, but with highly isotropic characteristics: the *lateral etch rate* is about 35% of the vertical etch rate, corresponding to an anisotropy factor <0.65.

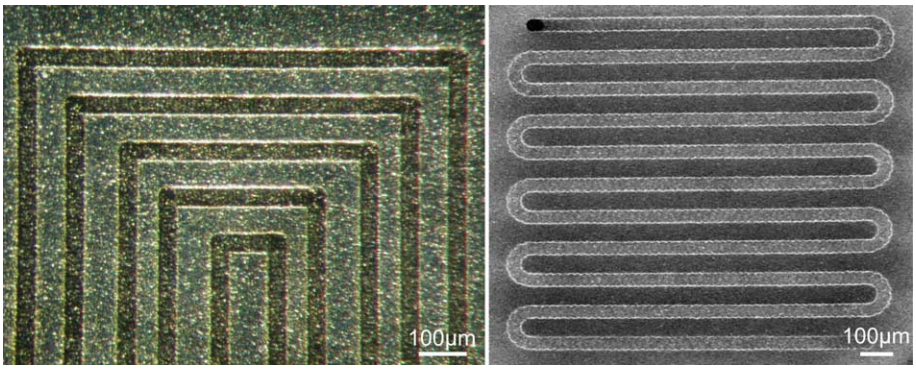

Fig. 2. Laser-written linear and circular line patterns in Al on GC (Left: microscope image. Right: SEM micrograph).

At lower pressures, reduced lateral etch rates and hence higher aspect ratios can be achieved: with a pressure of 60 mTorr, a vertical etch rate of 17.5 µm/h is reached with an anisotropy factor of about 0.72 (lateral etch rate about 4.8 µm/h, ~27% of vertical etch rate).

A second process is the *mask recession* that influences the observed lateral etch rate. The width of the written lines increases during etching, as lateral etching of the mask edges occurs at all pressures. The lateral etch rate under the mask is about 35% at 100 mTorr and 27% at 60 mTorr on each side of the mask. As the mask recession effect is more pronounced at lower pressures (~5% at 100 mTorr vs. ~19% at 60 mTorr), it partly compensates the lower lateral etch rate under the mask. Due to these different mechanisms, channels etched at lower pressure have a trapezoid cross-section, whereas channels etched at higher pressure exhibit curved walls and more isotropic characteristics.

An important aspect in reactive ion etching is often the formation of "grass" during the process, which impedes further etching. "Grass" is the term describing needle-shaped structures in the etched area resulting from residues on or in the etched material that locally impedes the etching process. This grass formation is also known as "micro masking effect" [20]. In the following, this expression is generally used for non-etchable material that remains in the etched region, even if the source and the properties of this material are very different.

During the reactive ion etching of glassy carbon in oxygen, two different types of "grass" were observed, depending on the material used as RF electrode cover. The glass cover leads to the formation of brittle white "flakes" in the etched regions, which do not significantly reduce the etch rate during the first 3 h of etching. These flakes can be assigned to glass sputtered from the RF electrode cover onto the sample. XPS studies have shown an amount of up to 10% of silicon, most probably in the form of SiO_2, on the sample surface. In the case of the metal cover a pronounced formation of a dense grass layer is observed, which severely inhibits the etching. A test performed with equal samples etched for 150 min at 50 mTorr, 150 W, and 5 sccm O_2 has shown that the etch rate with the metal electrode is only 40% of the etch rate achieved with the glass cover (17 vs. 7 µm/h).

An improved etch rate can probably be achieved by other etch systems with ICP (inductively coupled plasma) or ECR (electron cyclotron resonance) sources which should allow much higher etch rates due to the enhanced plasma density, lower mask wear due to lower bias voltage and reduced

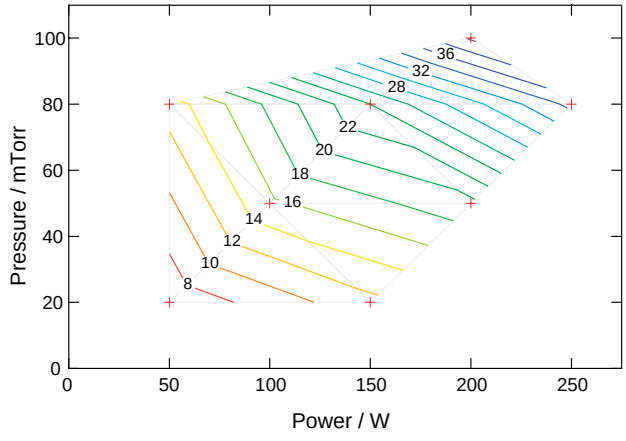

Fig. 3. Etch rates of GC plotted as a function of power and pressure. Crosses indicate measured data points, the lines labeled with numbers are lines of constant etch rate [µm/h] interpolated by a Delaunay triangulation algorithm.

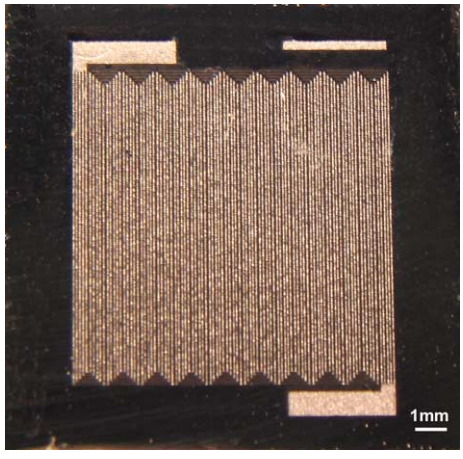

Fig. 4. Micro fuel cell electrode (14×14 cm^2) with 1 cm^2 meander flow field.

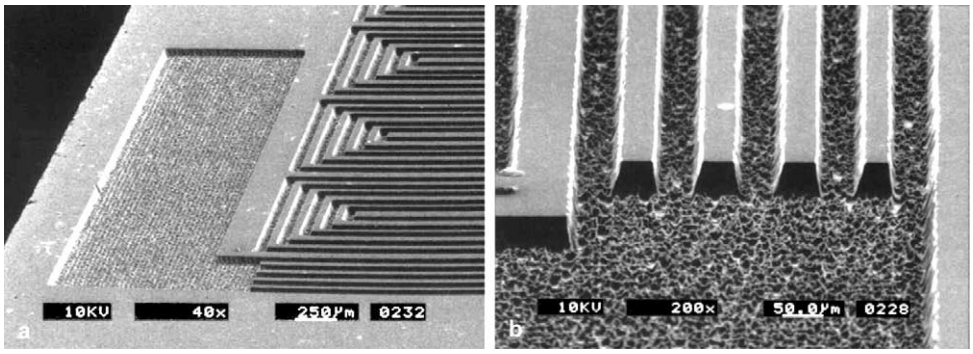

Fig. 5. SEM micrographs of channel structure with trapezoid cross-section and high roughness.

lateral etching due to operating pressures which are one order of magnitude lower than in our RIE system.

3.4. Achieved structure and application

Various flow field patterns have been fabricated with our combined laser-ablation and RIE process. In Fig. 4, a substrate of 14×14 cm^2 with a pattern of 5 parallel channels, meandering 19 ways across the active area of 1 cm^2, is shown. The line pitch is 100 µm, with a channel length of ~20 cm each. The gas feedthrough regions have a size of about 1×3.2 mm, and the via holes connecting these regions with the external gas source are prepared by electro discharge machining (not shown in Figs. 4 and 5).

In the micrographs (Fig. 5a and b) one can clearly see the high roughness, with r_a ~2.6 µm, and the trapezoid cross-section. For micro fuel cell applications, these structures are subsequently sputter-coated with platinum as the electro catalyst. The sloped walls could be beneficial for the sputter coating process, but the achievable aspect ratio is limited.

Micro flow fields structured by laser direct ablation have already been tested in a micro fuel cell setup and the characterization of reactive ion etched flow fields is currently in progress. Tests will show if the size of the electrochemically active surface area is sufficient for fuel cell operation or if other deposition methods yielding larger surface areas must be employed. The flow field layout (number of channels and meanders) and its depth will also be studied and optimized for the best performance.

4. Conclusion

Micro flow fields were successfully fabricated by the combination of the flexible laser mask patterning with reactive ion etching, which allows parallel pattern transfer of many samples. Complex structures for micro fuel cells and other applications can be easily fabricated with this process.

Laser mask writing is a very convenient rapid prototyping method and the important ablation parameters have been identified. The reactive ion etching step has been optimized for the available setup, but the aspect ratio is limited at acceptable etch rates. Other plasma etching systems could result in much higher etch rates and aspect ratios.

References

[1] S. Motokawa, M. Mohamedi, T. Momma, S. Shoji, T. Osaka, Electrochem. Commun. 6 (6) (2004) 562.
[2] J. Yu, P. Cheng, Z. Ma, B. Yi, Electrochim. Acta 48 (11) (2003) 1537.
[3] J.R. Yu, P. Cheng, Z.Q. Ma, B.L. Yi, J. Power Sources 124 (1) (2003) 40.
[4] S.J. Lee, A. Chang-Chien, S.W. Cha, R. O'Hayre, Y.I. Park, Y. Saito, F.B. Prinz, J. Power Sources 112 (2) (2002) 410.
[5] S.C. Kelley, G.A. Deluga, W.H. Smyrl, Electrochem. Solid-State Lett. 3 (9) (2000) 407.
[6] S.C. Kelley, G.A. Deluga, W.H. Smyrl, AIChE J. 48 (5) (2002) 1071.
[7] S. Tanaka, K.S. Chang, K.B. Min, D. Satoh, K. Yoshida, M. Esashi, Chem. Eng. J. 101 (1–3) (2004) 143.
[8] J.S. Wainright, R.F. Savinell, C.C. Liu, M. Litt, Electrochim. Acta 48 (20–22) (2003) 2869.
[9] R. O'Hayre, D. Braithwaite, W. Hermann, S.J. Lee, T. Fabian, S.W. Cha, Y. Saito, F.B. Prinz, J. Power Sources 124 (2) (2003) 459.
[10] U.A. Paulus, Z. Veziridis, B. Schnyder, M. Kuhnke, G.G. Scherer, A. Wokaun, J. Electroanal. Chem. 541 (2003) 77.
[11] M. Kuhnke, T. Lippert, E. Ortelli, G.G. Scherer, A. Wokaun, Thin Solid Films 453–54 (2004) 36.
[12] T. Lippert, A. Wokaun, Chimia 55 (10) (2001) 783.
[13] Y. Sohda, D.M. Tanenbaum, S.W. Turner, H.G. Craighead, J. Vac. Sci. Technol., B 15 (2) (1997) 343.
[14] S. Ssenyange, J. Taylor, D.J. Harrison, M.T. McDermott, Anal. Chem. 76 (8) (2004) 2393.
[15] G.K. Kiema, S. Ssenyange, M.T. McDermott, J. Electrochem. Soc. 151 (2) (2004) C142.
[16] O.J.A. Schueller, S.T. Brittain, G.M. Whitesides, Sens. Actuators, A, Phys. 72 (2) (1999) 125.
[17] O.J.A. Schueller, S.T. Brittain, G.M. Whitesides, Adv. Mater. 9 (6) (1997) 477.
[18] C. Eisenmenger-Sittner, E. Neubauer, C. Schrank, J. Brenner, C. Tomastik, Surf. Coat. Technol. 180–81 (2004) 413.
[19] K.E. Mayerhofer, E. Neubauer, C. Eisenmenger-Sittner, H. Hutter, Anal. Biochem. 374 (4) (2002) 602.
[20] K. Richter, M. Orfert, S. Howitz, S. Thierbach, Surf. Coat. Technol. 119 (1999) 461.